Journal of Ship Research, Vol. 45, No. 4, Dec. 2001, pp. 302–314

Experimental Validation of a Quasi-Explicit Hydrodynamic Model: Fishtailing Instability of a Single-Point Moored Tanker in Rigid-Hawser Configuration

E. A. Tannuri,[*] **A. N. Simos,**[†] **A. J. P. Leite,**[‡] and **J. A. P. Aranha**[*]

[*] *Department of Mechanical Engineering, USP, S.P., Brazil*
[†] *Department of Naval Architecture and Ocean Engineering, USP, S.P., Brazil*
[‡] *E&P, Petrobras, R.J., Brazil*

The extended hydrodynamic model derived in Simos et al (2001), where the yaw velocity terms have been incorporated to the model proposed by Leite et al (1998) while preserving its quasi-explicit feature, is used here to study some typical dynamic problems of moored ships, specifically the fishtailing instability that may occur in a single-point mooring (SPM) system. Since the intention was to check the hydrodynamic model, the hawser was assumed rigid to avoid the complex dynamics that may occur when the actual hawser slackens and the obtained results were confronted with experimental ones, obtained at the IPT wave tank. The agreement is very good in the sense that not only the limit-cycle amplitudes are compatible but also the time series are very similar. For the VLCC model in ballasted condition (40%) the fishtailing instability occurs only for a relatively high current velocity and some Froude effect is then detectable. Using results from the static bifurcation experiment an *ad hoc* correction is proposed for such effect, showing a relatively close agreement between experiments and the theoretical model. This Froude effect correction is, however, not relevant for an actual SPM system subjected to a usual ocean current.

1. Introduction

In the analysis of a moored ship exposed to an ocean current, two sorts of approaches have generally been followed in the literature: the first, based on the classic work by Abkowitz (1964), addresses the problem by experimentally obtaining the hydrodynamic derivatives for low velocities (see Takashina (1986) and Fucatu & Nishimoto (1998), for example); the second, described for instance in Obokata (1987), adjusts the static force coefficients to incorporate the influence of the yaw angular velocity and it has been adopted by several commercial programs such as Dynfloat (Marin), Simo (Marintek) and Ariane (Bureau Veritas). What differs one program from the other is, in essence, the choice of the coefficients and their experimental sources. What renders difficult their utilization is the uncertainty about the values of such coefficients for an actual ship and how one should extrapolate them from model-scale to full-scale. Wichers (1987), for example, does not predict any scale correction for the force coefficients, even for the surge component, and his work seems to be the basis of the Dynfloat program.

A third route, less empirical and more theoretically oriented, starts with some well-defined hydrodynamic model (short wing theory for a flat plate) and, based on a large statistical analysis of experimental results, makes some adjustments taking into account the ship's main dimensions. This approach, suggested for instance by Clarke et al (1982), was originally intended to furnish a quick estimate of the linear hydrodynamic derivatives, but it has been gaining some support lately. At least in some aspects the paper by Oltmann & Sharma (1984) can be placed in this category and the one written by Leite et al (1998) is certainly well rooted in Clarke's work. Simos et al (2001) proposed an extension of Leite's work by incorporating the dynamic parcels, related to the yaw angular velocity. The final model, synthesized by expressions

Manuscript received at SNAME headquarters August 9, 2000; revised manuscript received June 1, 2001.

(1) and (14) of their paper, will be coined here "USP model" in order to make the notation shorter.

As explained in Simos et al (2001), their work aimed to derive a hydrodynamic model with the following features. First, it should have a clear *physical background*, in such a way that the dependence on scale-factors (Reynolds number Re) is well-defined. Second, the model should be *quasi-explicit* or, in other words, a function of some few hydrodynamic coefficients which could be relatively well estimated by standard means. Finally, the model should be able to adequately predict the current effects acting on the ship hull for the context it was derived, namely, the hydrodynamic analysis of moored tankers.

The first two attributes were well established for the USP model in Simos et al (2001): the derived model has indeed a clear physical background and depends only on the ship's main dimensions and on a small set of hydrodynamic coefficients that can be easily estimated, both at model and full-scale dimensions. Furthermore, there is a close agreement between the predicted forces and those measured in several yaw rotating tests performed at IPT and Marin. The verification of the third attribute is the basic purpose of the present work.

The idea here is that such a simple hydrodynamic model should not, in principle, be able to cope with the totality of possible applications but it must be well fitted for the specific purpose it has been derived: in the present case, the analysis of moored tankers. One should then look for a well-defined test situation, both typical and demanding for the model, to check whether or not it has a predictive capability and, also, to disclose the parameters that are really relevant in the given situation, namely, the parameters that affect more strongly the response of the system.

For the problem under analysis the most conspicuous dynamic phenomenon is, certainly, the so-called *fishtailing instability* of a single-point moored tanker. In this case, the trivial equilibrium position, where the ship is aligned to the ocean current, becomes unstable and the ship then performs an oscillatory motion on the horizontal plane (limit-cycle). In reality, the dynamic behavior can become much more complex since the hawser that joins the ship to the fixed point can slacken, sometimes causing a chaotic response of the whole system. This latter feature, however, is not hydrodynamic in essence since it depends mainly on the unilateral response of the hawser, and the intention here is to verify specifically the hydrodynamic model and not the actual coupled ship-hawser dynamic behavior.

For this reason, a particular experimental setup was used in this work[1]: a tanker moored in a single point by a *rigid hawser* while exposed to a uniform current; see Fig. 1. This situation can be simulated in a wave tank by towing the mooring point with constant velocity U and, in doing so, the unnecessary complexities related to the eventual slacking of an actual hawser are avoided. At the same time, the richness of the dynamic phenomenon is partially preserved, at least, being caused mainly by the nonlinearities of the hydrodynamic forces.

Since the hawser is rigid, the dynamics of the ship-hawser system can be entirely described by two dynamic variables: the angle $\gamma(t)$ between the hawser and the towing direction and the heading angle $\psi(t)$. There are two geometric control parameters: the hawser's length L_b and the position aL where the articulation is placed on the ship, L being the ship's length. In general, the heading angle $\psi(t)$ is small and it is then clear, from Fig. 1, that the ship-hawser system is similar to a pendulum, the friction force on the ship's hull playing the role of the gravity. It turns out that a third parameter, this one hydrodynamic, also controls the system response: the friction coefficient $C_f(\mathrm{Re})$, where $\mathrm{Re} = UL/\nu$.

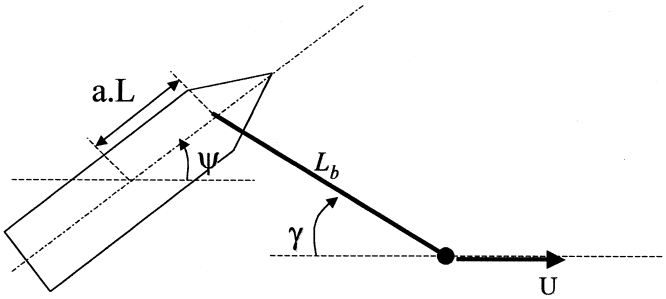

Fig. 1 Schematic representation of fishtailing instability with *rigid hawser.* L_b = hawser length; aL = articulation position; $(\gamma(t); \psi(t))$ = dynamic variables

It is evident thus, from the outset, that the fishtailing instability phenomenon is strongly scale-dependent, since it is a function of the friction coefficient $C_f(\mathrm{Re})$. In particular, experimental results obtained with small-scale models in a wave tank cannot be directly extrapolated to the full-size scale. One must, therefore, rely entirely on the mathematical model to infer the behavior of the actual full-scale system and such model must then be able to describe the scale-effects in a proper manner. In this perspective, the purpose of making experiments in a wave tank is to assert, first, the ability of the mathematical model to predict this small-scale situation and, second, to check its sensibility to variations of $C_f(\mathrm{Re})$. Once these goals are fulfilled, the confidence in the mathematical model as an extrapolator is certainly enhanced if the model has a simple texture and the physical background can be easily recognized, two attributes shared by the USP model.

For a given position of the articulation (fixed aL) the fishtailing instability problem depends only on two parameters: the hawser's length, through the parameter L_b/L, and the towing velocity U, through the friction coefficient $C_f(\mathrm{Re})$. By changing these parameters in a relatively wide range, a variety of instability situations can be covered, both experimentally and numerically, and the adequacy of the mathematical model can then be verified.

This direct simple experimental approach faces, however, some technical difficulties that are worth to be commented upon here: in fact, for VLCC1 with main parameters defined in Simos et al (2001), the velocity $U = 0.2$ m/s at the model scale corresponds, roughly, to an ocean current of 4 knots in reality and to a cross-section Froude number $U/(gB)^{1/2} = 0.08$. To emulate a real situation one would like to cover the range 0.1 m/s $\leq U \leq$ 0.2 m/s but, at such low velocities, the fluid forces at the model scale are so small that unavoidable mechanical friction in the articulations interferes with them. Furthermore, as it will be shown, the VLCC1 in ballasted condition (40%) is *stable* for $U \leq 0.2$ m/s, irrespective of the value of L_b/L. Both circumstances have pushed the experiments to the range 0.4 m/s $\leq U \leq$ 0.6 m/s but then a second concern arises: the cross-section Froude number becomes relatively large, falling in the range $0.16 \leq U/(gB)^{1/2} \leq 0.24$. For such values, some Froude effect on the lateral force and

[1]The experimental setup was suggested, independently, by one of the authors (A. J. P. Leite) and by Prof. Sergio Sphaier.

Table 1 Friction coefficient C_f(Re) at the model scale. VLCC1 in the *loaded condition* (100%)

U(m/s)	Experiments—IPT	ITTC*
0.4	0.0223–0.0247	0.0216
0.5	0.0211–0.0227	0.0206
0.6	0.0199–0.0207	0.0199

*Calculated with ITTC friction line, form factor $k = 0.25$ (see Simos et al (2001)).

yaw moment should be expected but those are nonmodeled influences in Simos et al (2001). In reality, as will be seen, this Froude effect, although nearly irrelevant in the loaded condition (100%), becomes appreciable in the ballasted condition (40%) and a sort of *ad hoc* correction should then be provided.[2]

The work has thus been organized in the following way: in Section 2 some experimental and theoretical results, not directly related to the fishtailing instability experiments but relevant for their interpretation, are presented and discussed. In particular, the assessment of the Froude effect on the yaw moment is elaborated and an *ad hoc* correction for the ballasted condition is proposed. In Section 3 the fishtailing instability experiments and the numerical results from the USP model are compared for the loaded condition of VLCC1 and, in Section 4, the same comparison is made for the ballasted condition, including then the *ad hoc* correction for the Froude effect on the yaw moment. Section 5 presents the conclusion of this work.

2. Friction force, stability and Froude effect

The measurement of the friction coefficient at the model scale in low velocities is technically difficult since the global force is small. Some spread in the measured values seems to be unavoidable and Table 1 gives the values obtained at IPT for VLCC1 in the loaded condition; for reference, the values from the ITTC curve, see (6) in Simos et al (2001), are also given. Note that the longitudinal Froude number is indeed small $(U/(gL)^{1/2} < 0.1$ for $U \leq 0.6$ m/s) and the Froude effect on the longitudinal force can, in principle, be disregarded. The results for the ballasted condition (40%) are shown in Table 2.

Given the dynamic system defined by (1) & (14) in Simos et al (2001), the *stability* of the *trivial solution* $\{u(t) = U; v(t) = r(t) \equiv 0\}$ can be studied by linearizing the set of dynamic equations in its vicinity. As discussed in the Introduction, there are three parameters that control the dynamic behavior of the system and so the stability conditions: the articulation position aL, the hawser length L_b/L and the friction coefficient C_f(Re). For a fixed aL the stability region can be drawn in the parameter plane $(C_f; L_b/L)$, the results for VLCC1, both in loaded and ballasted conditions, being shown in Fig. 2. The curve separating stable from unstable regions in the plane $(C_f; L_b/L)$ has been coined *threshold line* and, in all experiments to be shown in Sections 3 and 4, the values of a are exactly the ones indicated in Fig. 2: $a = 0.5$ for 100% and $a = 0.4$ for 40%.

In Fig. 2 the values of C_f for the corresponding velocities are the ones measured at IPT, see Tables 1 and 2. The stability is, in general, recovered for L_b/L large enough, as shown in curve (b) of Fig. 2 and also suggested by some experimental results, see Section 3.

The *ballasted condition* is stable for $U = 0.2$ m/s even if the value of C_f is taken according to the ITTC curve ($C_f = 0.041$). A similar conclusion can be inferred from the experimental results: apparently,[3] the initial oscillation sets down (stability condition) when the ship is in the ballasted condition and $U = 0.2$ m/s, in accordance with the theoretical result shown in Fig. 2; see Fig. 3, for example. In all tests, the angular instrumentation precision is approximately ± 0.4 deg.

Hopf bifurcation (see Tabor (1989)) is the rule for the unstable regions presented in Fig. 2, indicating that in such regions a *limit-cycle* ("fishtailing" in the naval engineering nomenclature) is obtained. The mathematical model predicts, however, that the type of bifurcation is modified as the articulation approaches the midsection ($a \to 0$), changing to a *static bifurcation* for aL small enough: in this case the ship finds another static stable equilibrium position with $(\gamma \neq 0; \psi \neq 0)$, similar to the static bifurcation analyzed in Leite et al (1998) for a turret configuration.

This conclusion is supported by experiments on the ship-hawser system of Fig. 1: for the VLCC1 in ballasted condition and $a = 0.2$ it can be clearly observed that $\gamma(t) \to \gamma_0 \neq 0$; $\psi(t) \to \psi_0 \neq 0$; $F_H(t) \to F_{H,0} \neq R$, where $F_H(t)$ is the axial force on the rigid hawser and R is the frictional resistance of the ship. Figure 4 displays a typical experimental result in this situation, showing the asymptotic stability of the (bifurcated) equilibrium $(\gamma_0; \psi_0)$. Notice the qualitative change of behavior between Fig. 3, where $a = 0.4$, and Fig. 4, where $a = 0.2$. Also, the angle γ_0 is defined by the condition that the hawser be aligned with the resultant of the hydrodynamic forces on the ship hull. The hawser force, measured with strain gages, shows a typical high-frequency noisy oscillation even in this quasi-static problem. In all tests, the force instrumentation precision is approximately ± 20 gf.

In the *static bifurcation* the stable equilibrium yaw angle ψ_0 depends only, for a given a, on the transverse (sway) force and the yaw moment, being completely independent of the surge force and therefore of the friction coefficient C_f(Re). It follows that ψ_0 should, within the context of the proposed model, be independent of the velocity U. Nevertheless, as observed in Leite et al (1998) and also in the present set of experimental results, the equilibrium value ψ_0 seems to increase monotonically with U.

Table 2 Friction coefficient C_f(Re) at the model scale. VLCC1 in the *ballasted condition* (40%)

U(m/s)	Experiments—IPT	ITTC*
0.4	0.0354–0.0392	0.0352
0.5	0.0335–0.0352	0.0336
0.6	0.0320–0.0329	0.0324

*Calculated with ITTC friction line, form factor $k = 0.25$ (see Simos et al (2001)).

[2]Notice, however, that in a real situation the cross-section Froude number is, in general, smaller than 0.08 and no Froude correction is needed, both for loaded and ballasted conditions.

[3]In the *stable* vicinity of the *threshold line*, as for the case $U = 0.2$ m/s in the ballasted condition, the damping factor is very small and the decay time is very long; it turns out then that a stable behavior can be strictly confirmed only for a very long wave tank. IPT wave tank has a length of 160 m, still a little bit short for this purpose.

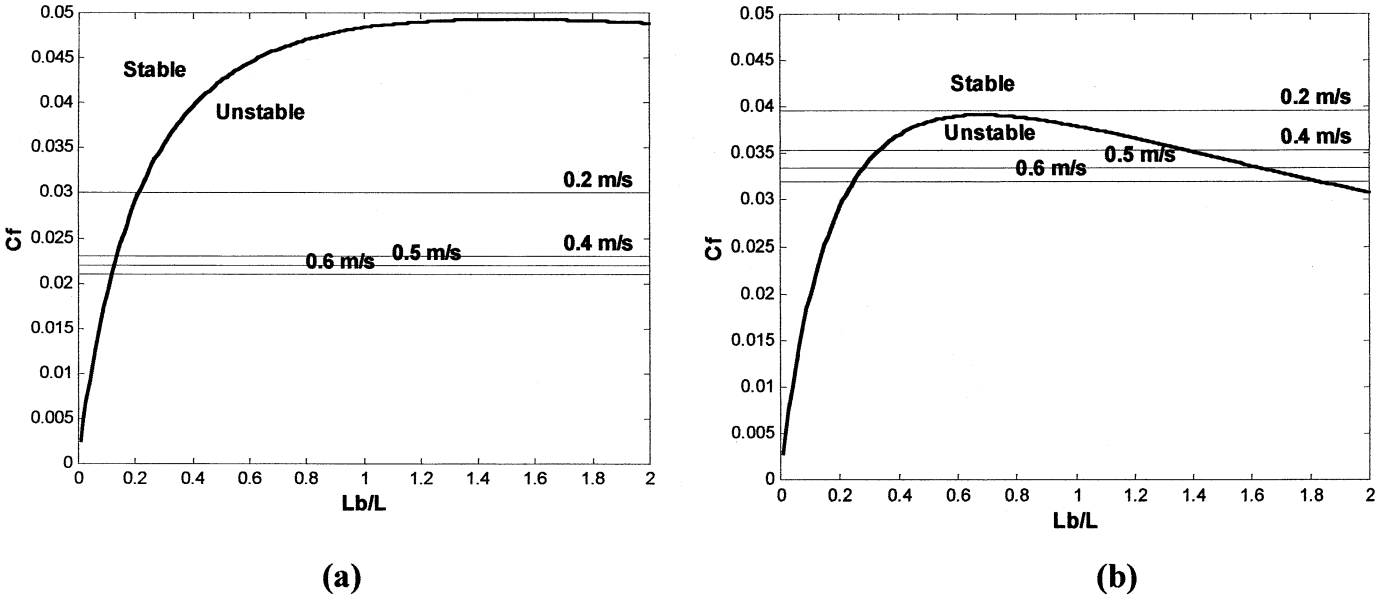

Fig. 2 Stability region for the ship-hawser system of Fig. 1—USP model. (a) VLCC1(100%); $a = 0.5$; (b) VLCC1 (40%); $a = 0.4$

Figure 5 displays such result in a very clear manner: using the USP model, the bifurcation curve $\psi_0 \times aL$ was drawn for VLCC1 in ballasted condition and compared with experimental results. For $a = 0.2$ and $U = 0.2$ m/s there is, indeed, a close agreement between theory and experiment. For higher velocities, however, the equilibrium values ψ_0 are much larger, showing a tendency to increase with U. Since the mathematical model predicts that such angle should be independent of the velocity, the observed behavior could only be due to some *nonmodeled effect*, the waves generated at the free-surface (Froude effect) being the most likely candidate.

A simple approach to estimate the free-surface influence can be tentatively addressed in the following way: First, in order to render easier the analysis, among the two transverse forces (sway force and yaw moment), only one of them will be selected to incorporate the Froude effect; second, this influence should appear as a multiplicative factor on the related force coefficient. In the bifurcation analysis of a ship articulated at $0.2L$ the yaw moment is the prominent transverse force and it was thus selected to incorporate the Froude effect; so, the static yaw moment coefficient (C_{6C}) of the USP model (see (5) in Simos et al (2001)) can be rewritten in the form

$$C_{6C}^{(FE)}(\psi) = C_{6C}(\psi) \cdot [1 + k_w(\mathrm{Fr}; \psi)] \tag{1}$$

where the yaw angle ψ is used here instead of the incidence angle $\alpha = \pi - \psi$.

The Froude correction factor $k_w(\mathrm{Fr}; \psi)$ should become more relevant when the yaw angle increases, although this dependence is difficult to be evaluated, and Table 3 gives the estimated correction factor in order that the experimental points of Fig. 5 be fitted by the mathematical model. Notice that for 0.4 m/s $\leq U \leq$ 0.6 m/s the yaw angle is in a range around $\psi \approx 17.5$ deg and the *ad hoc* expression (1) with $k_w(\mathrm{Fr}; \psi)$ given in Table 3, can possibly be used for a similar range of values of the yaw angle. The curve labeled $U = 0.4$ m/s in Fig. 5 gives the bifurcation curve when USP model is corrected by Froude effect accordingly to (1) and Table 3.

The same procedure can also be used for the loaded condition and Table 4 gives the related correction factor for this case. Note that now the correction factor $k_w(\mathrm{Fr}; \psi)$ is much smaller than in the ballasted case, despite the fact that the typical yaw angle is now $\psi \approx 35$ deg, twice the value of the typical ψ observed in the ballasted condition.

As will be seen in the following sections, the amplitudes of the experimentally measured yaw angles in the fishtailing instability phenomenon remain in a range between 10 deg and 20 deg, at the same level of the bifurcation angles observed in the ballasted condition but much smaller than the ones observed for the loaded ship. It seems reasonable then to use (1), with values from Table 3, for the ballasted condition but the same conclusion cannot be extended to the loaded situation: here the Froude effect should be smaller than the already small values of Table 4 since these values are obtained for yaw angles around 35 deg, roughly twice the ones observed in the fishtailing instability experiments. It turns out, then, that the original USP model (without the Froude

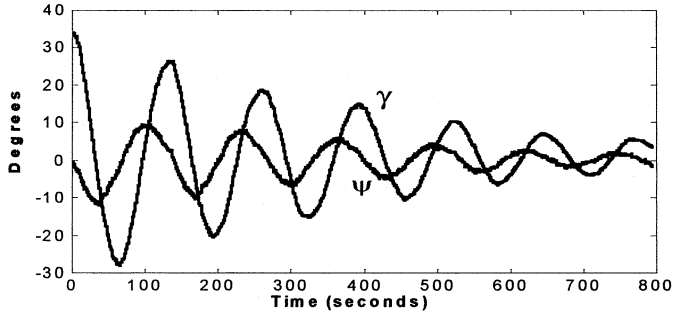

Fig. 3 Experimantal behavior of the ship-hawser system—IPT wave tank. (VLCC1(40%); $a = 0.4 - U = 0.2$ m/s; $L_b/L = 0.36$)

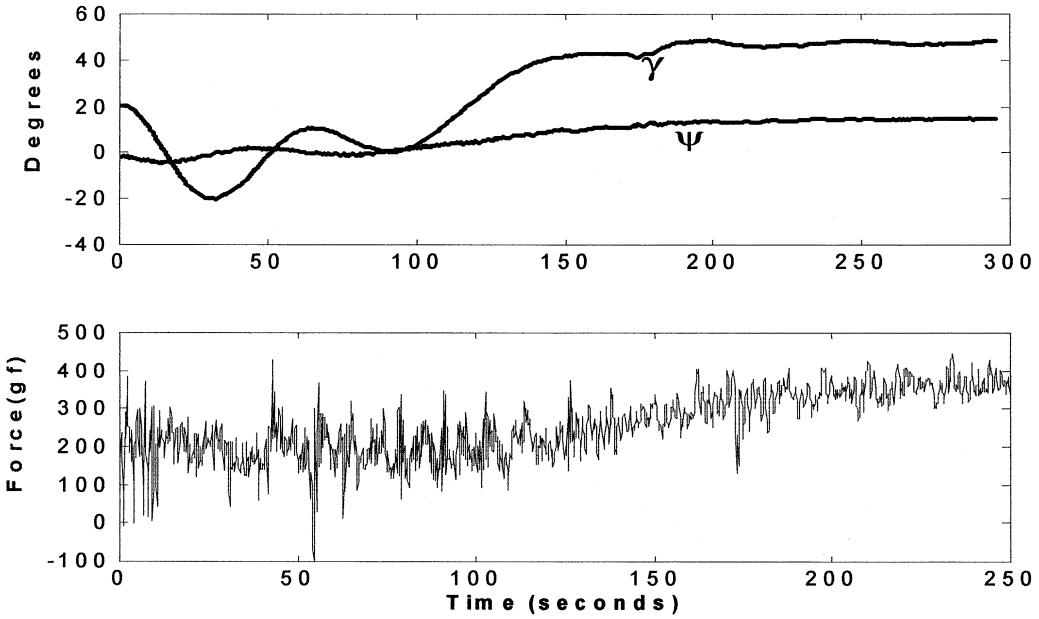

Fig. 4 Static bifurcation: Behavior of $(\gamma(t); \psi(t); F_H(t))$ for VLCC1—IPT wave tank. ($U = 0.5$ m/s; $L_b/L = 0.287$—ballasted condition: $a = 0.2$)

correction) can be used in the loaded condition but, in the ballasted situation, one must employ (instead of $C_{6C}(\psi)$) the yaw coefficient corrected by the Froude effect, according to (1) with $k_w(\mathrm{Fr}; \psi)$ from Table 3. This procedure is followed throughout Section 4.

3. Fishtailing instability experiment—loaded condition

In the fishtailing instability experiments of the ship-hawser system defined in Fig. 1 a small-scale physical model of VLCC1 was used, both at the loaded (100%) and ballasted conditions (40%). The scale factor is $\lambda = 90$ and the relevant parameters of VLCC1 −100% are defined in Table 3 of Simos et al (2001). It should be observed, in particular, that for the whole set of numerical simulations to be presented in this section (and also those presented in Section 2) the values $\{C_Y = 0.78; lC_Y = 0.035\}$, obtained from Hoerner's curve and Table 1 in Simos et al (2001), were used instead of the measured values $\{C_Y = 0.87; lC_Y = 0.045\}$. Simulations of the fishtailing instability phenomenon with the measured values were also performed but the final results could not be differentiated from the ones computed with the estimated values. This result implies, first, that this phenomenon is

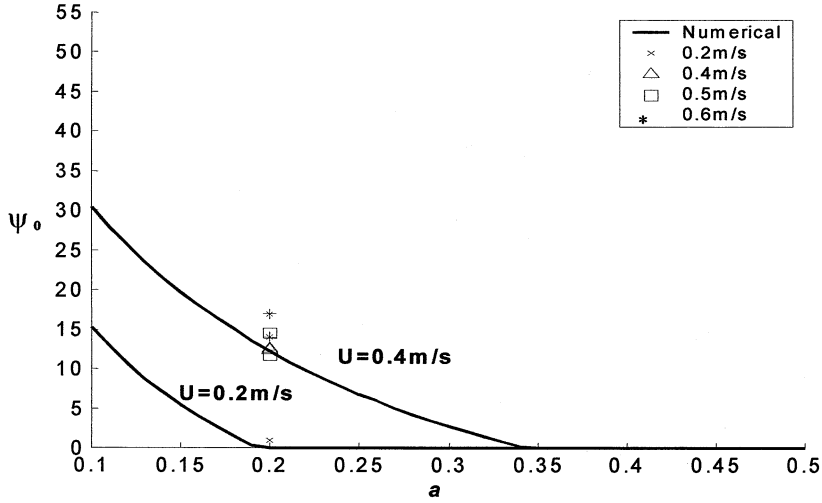

Fig. 5 Bifurcation curve for VLCC1 in the ballasted condition—a = bifurcation parameter. $U = 0.2$ m/s: USP model; $U = 0.4$ m/s: USP model with Froude effect (see (1))

Table 3 *Ad hoc* Froude correction factor—static bifurcation. (VLCC1 in ballasted condition 40%; $a = 0.2 - \psi \approx 17.5$ deg)

U(m/s)	k_w(Fr; ψ)
0.2	0
0.4	0.77
0.5	0.82
0.6	1.03

reasonably insensitive with respect to variations of $\{C_Y; lC_Y\}$ at least within this range and, second, that the so called *explicit model*, where the few hydrodynamic coefficients of the USP model are inferred from known results of ship hydrodynamics, can be used in the analysis of a moored tanker. However, as discussed below, a fine-tuning between experiments and theory is very much dependent on the friction coefficient C_f(Re).

The typical frequency scale in the ship-hawser system of Fig. 1 is $\omega \approx U/L$ and so the oscillation period is of the order $P \approx 2\pi \cdot L/U$. If L_{WT} is the wave tank length, the number N of complete oscillations in one run should be of order $N \approx 1/2\pi \cdot L_{WT}/L \approx 7$, since $L_{WT} = 160$ m in IPT wave tank and $L = 3.56$ m. This estimative is close to what is observed for the towing velocity $U = 0.2$ m/s (see Fig. 2) but the pendulum analogy suggests that the period should increase with the towing velocity since the "gravity" C_f(Re) decreases with it. This was indeed verified in the experiments since no more than four complete oscillations could be observed for 0.4 m/s $\leq U \leq$ 0.6 m/s. It follows that if the experiment were started with the ship and hawser aligned (trivial equilibrium position) there would not be enough length to fully develop the instability until the *limit-cycle* is settled. This is the reason why, in the figures to be shown, the initial state is, in general, of the form $(\gamma(0) \neq 0; \psi(0) \neq 0)$, in order to reach the *limit-cycles* faster. Perturbations on the initial conditions were also tested experimentally and in all situations the same limit was obtained, indicating at least a local attractive character of the limit-cycle solution.

Another point should be emphasized here. In the numerical simulations with the USP model the initial state is the same as in the experiments and the value of C_f(Re) was chosen, in general, not from the ITTC line but from the measured values of Table 1. Although the difference between both values is small, the period of the limit-cycle is very susceptible to the value of C_f(Re) and a small mismatch would turn difficult the visual comparison of the time series. Otherwise, from a more practical point of view, it makes no difference to take the friction coefficient either from experiments or from the ITTC curve and thus the USP model, in its explicit version, can be confidently employed to predict the behavior of a single point moored tanker.

Table 4 *Ad hoc* Froude correction factor—static bifurcation. (VLCC1 in loaded condition 100%; $a = 0.2 - \psi \approx 17.5$ deg)

U(m/s)	k_w(Fr; ψ)
0.2	0
0.4	0.12
0.5	0.17
0.6	0.31

The dynamic behavior of the ship-hawser system of Fig. 1 depends, as already said, on three parameters: the articulation position aL, the hawser length L_b and the towing velocity U (friction coefficient C_f(Re)). For the *loaded condition* the articulation was kept at the position $a = 0.5$ but the hawser length and towing velocity took the values $\{(U = 0.4$ m/s; 0.5 m/s; 0.6 m/s); $(L_b/L = 0.1; 0.2; 0.3; \ldots; 1)\}$, totaling 30 different experiments for the 100% condition.

Figures 6, 7 and 8 show typical results for the time series of the ship-hawser angular displacements $(\gamma(t); \psi(t))$ and also of the hawser force $F_H(t)$. Notice that the values of C_f(Re) used in the simulations correspond to the lower bounds of the experimental values of Table 2.1 and that they are not very far from those obtained by the ITTC curve. Being typical, as they are, the purpose to select just this set of experiments to be shown here has only one reason: in all of the figures the hawser lengths are the same and so the change in behavior is solely due to the friction coefficient. Besides the differences in the amplitudes of the limit-cycles when the towing velocity changes, it is important to call the attention to a more subtle aspect in these time series: in fact, while $\gamma(t)$ has a nearly "harmonic" form, the yaw angle $\psi(t)$ assumes a sort of "sawtooth" form that becomes "undulating" (at least in the first cycle) in the case $U = 0.6$ m/s, a kind of fine behavior very well captured by the USP model. In reality, this more undulating behavior is a *transient response* that depends essentially on the initial condition and, to a lesser extent, on the value of the friction coefficient.[4] Notice also that the sawtooth-like behavior is recovered in the plot of Fig. 9, where now $C_f = 0.021$ and the initial state for ψ is smaller.

As a last observation, the experimental hawser force signal presents, as already pointed out in Fig. 4, a high-frequency noise that tends to become less evident (the signal becomes cleaner) when the force increases with the velocity U. Nonetheless, the agreement between the mean values of the measured forces and their theoretical prediction is fair enough for the whole range of towing velocities.

Figure 10 shows a synthesis of the fishtailing instability study for the loaded situation. In this figure, the amplitudes of the limit-cycles of $\gamma(t)$ and $\psi(t)$ as a function of L_b/L, for the three different velocities, have been obtained through the USP model and compared with the experimental results. The values of C_f used in the simulations appear in the figure captions and a relatively close adherence is observed between theory and experiments, exception made to the small values of L_b/L: In these cases the dynamic system is in the vicinity of the *threshold line* of Fig. 2 and then, as a consequence, not only is the time scale to reach a steady-state larger but also the net destabilizing forces are smaller, possibly turning the global behavior more susceptible to the friction on the articulations. Notice also that the γ-amplitude tends to decrease with L_b/L, suggesting that the stability is eventually recovered for L_b/L large enough, a result supported by the stability analysis of the USP model. Figure 2 shows a similar result for the ballasted condition.

To finish this discussion, Fig. 11 shows the simulation, with the USP model, of two cases: one with $\{a = 0.5; L_b/L = 0.7; C_f = 0.023\}$, corresponding to the velocity $U = 0.4$ m/s in Fig. 6; the other with $\{a = 0.5; L_b/L = 0.7; C_f = 0.0074\}$, corresponding to

[4]For smaller friction coefficients ($C_f < 0.017$) the steady-state yaw angle becomes undulating, as shown, for example, in Fig. 11.

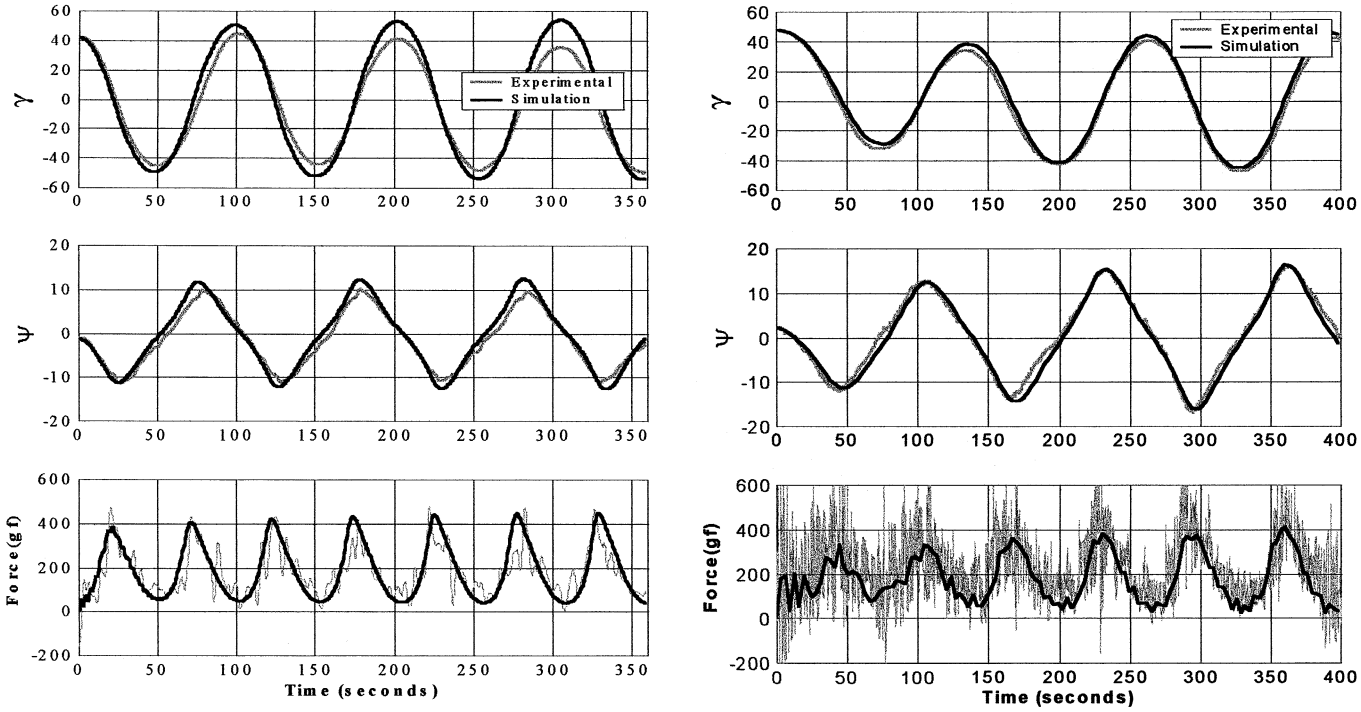

(U = 0.4 m/s; C_f = 0.0223; a = 0.5; L_b/L=0.36)

(U = 0.4 m/s; C_f = 0.023; a = 0.5; L_b/L=0.7)

Fig. 6 Fishtailing instability: theory and experiment. VLCC1 loaded (100%), $U = 0.4$ m/s

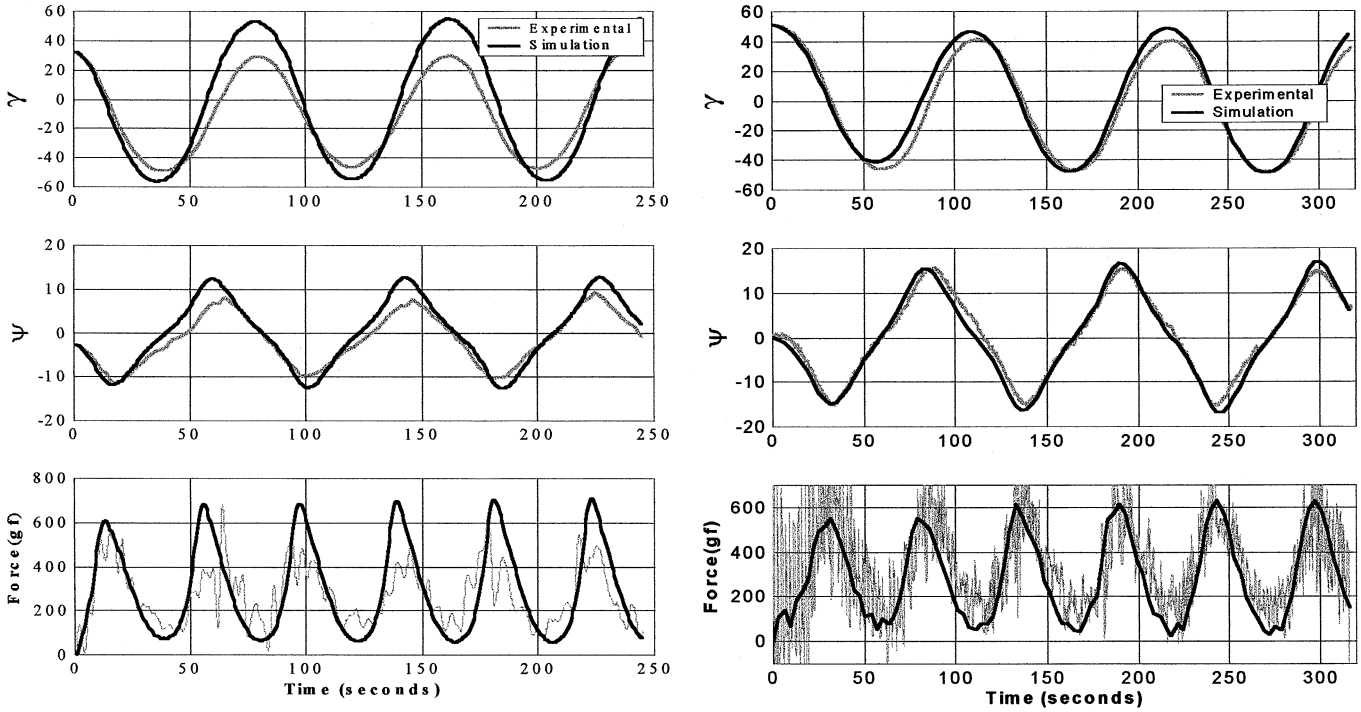

(U = 0.5 m/s; C_f = 0.022; a = 0.5; L_b/L=0.36)

(U = 0.5 m/s; C_f = 0.0211; a = 0.5; L_b/L=0.7)

Fig. 7 Fishtailing instability: theory and experiment. VLCC1 loaded (100%), $U = 0.5$ m/s

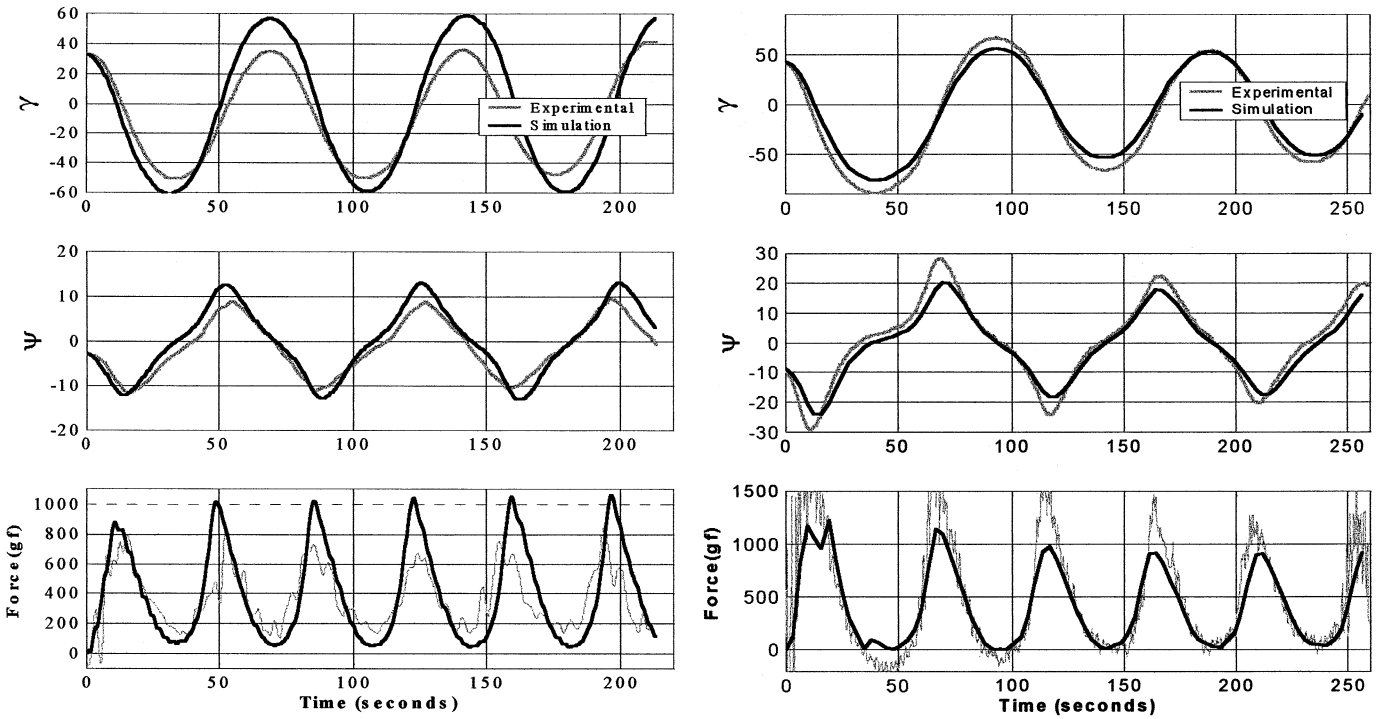

(U = 0.6 m/s; C_f = 0.0203; a = 0.5; L_b/L=0.36)

(U = 0.6 m/s; C_f = 0.0199; a = 0.5; L_b/L=0.7)

Fig. 8 Fishtailing instability: theory and experiment. VLCC1 loaded (100%), $U = 0.6$ m/s

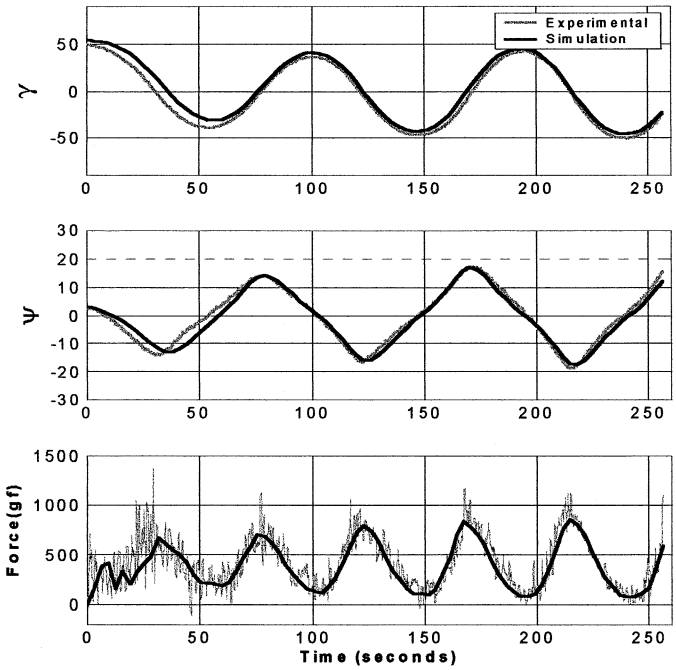

(U = 0.6 m/s; C_f = 0.021; a = 0.5)

Fig. 9 Fishtailing instability: theory and experiment. ($L_b/L = 0.8$)

the same problem in full-scale. Just to make direct the comparison, the time variable in full-scale was reduced by Froude law to the small-scale. It can be seen that the discrepancy between the two results is outstanding. In particular, by looking also to Fig. 6, it becomes clear why the small-scale experimental results for the fishtailing phenomenon cannot be extrapolated to full scale.

4. Fishtailing instability experiment—ballasted condition

One of the attributes of the hydrodynamic model proposed in Simos et al (2001), called here USP model, is its potential ability to deal with arbitrary ships, in different ballast conditions, without the need of more extensive experimental data for the related hydrodynamic coefficients. This goal is formally achieved by expressing the mathematical model directly in terms of the ship's main dimensions, the only geometric differences between the loaded and ballasted conditions relevant for the USP model being the draft T and the wetted surface S.

At least in the context of the overall force coefficients, the USP model has been tested against results from yaw rotating experiments showing an adequate concordance, both for the loaded and ballasted conditions (see Simos et al (2001)). It is thus expected that a similar agreement should be observed when checking the performance of the model in the fishtailing instability experiment defined in Fig. 1. However, as discussed in Section 2, some technical problems arise in this context. On the one hand, the stability

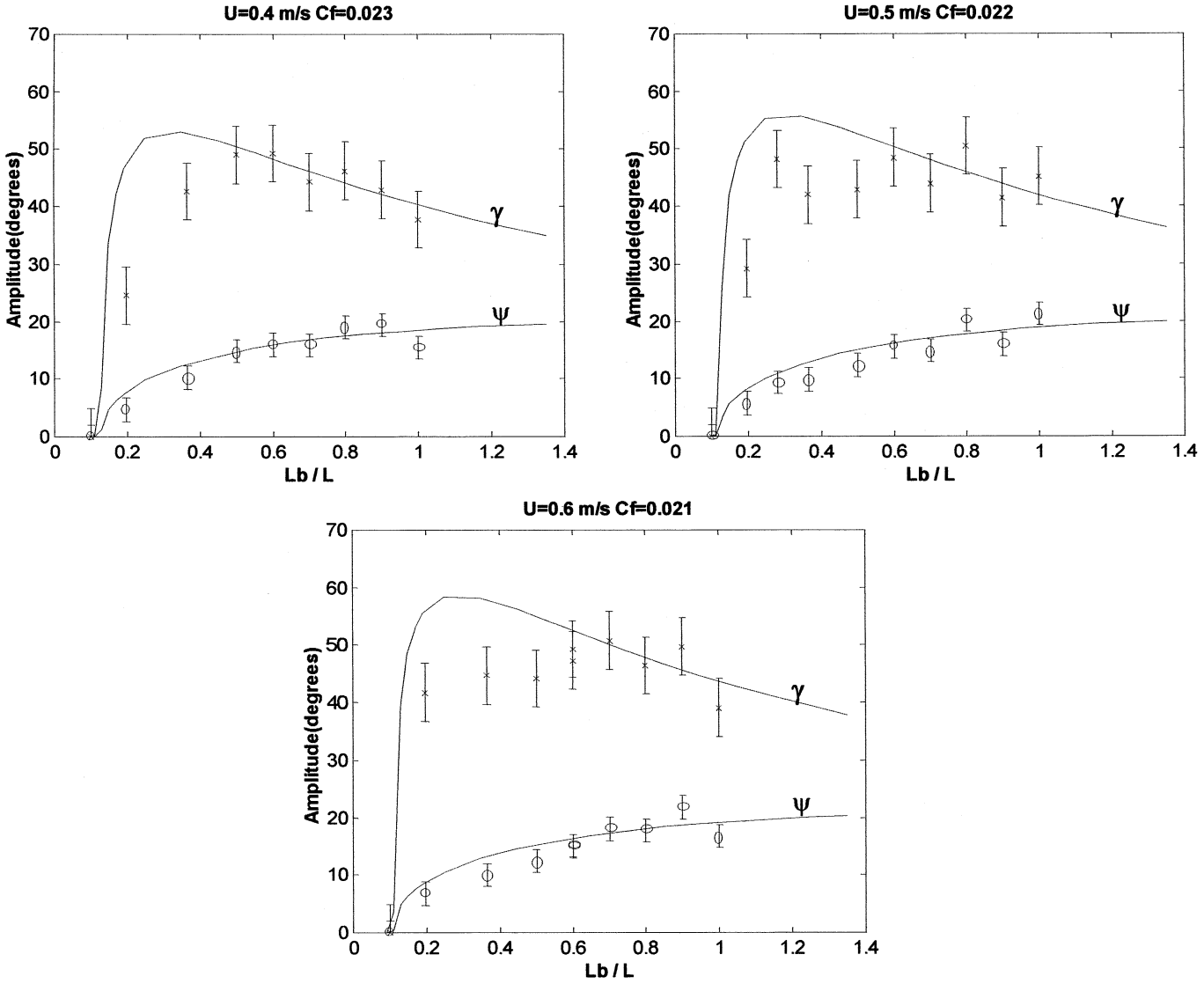

Fig. 10 Amplitude of the limit-cycles as functions of L_b/L—loaded situation. $(+) = \gamma(t)$—experiment; $(o) = \psi(t)$—experiment:(———)-USP model

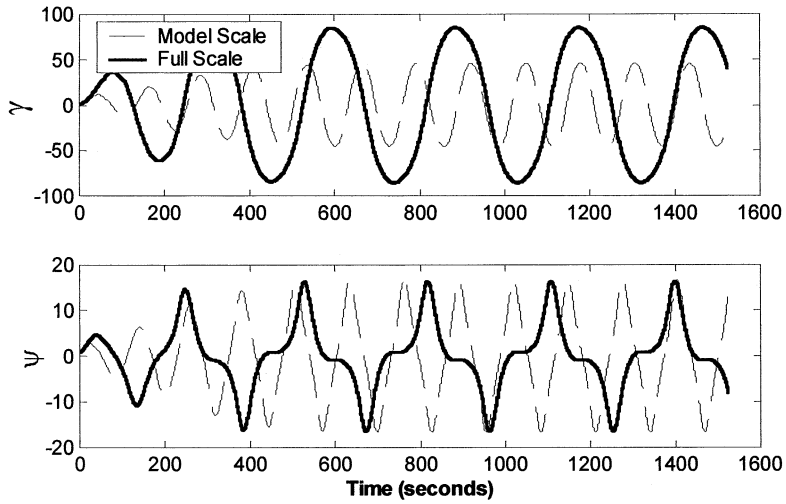

Fig. 11 Comparison between small and full scale at the same Froude number—USP model

study shows and the experiments confirm that only for velocities relatively higher than $U = 0.2$ m/s in the small-scale dimension the fishtailing instability can be developed for the ballasted case; on the other hand, the static bifurcation experiments indicate that Froude effect plays an important role for such high velocities and should not be ignored in the analysis. In the face of this dilemma, two options are left: either not to make the comparison for this condition or else to provide an *ad hoc* correction on the USP model, trying to incorporate the Froude effects. This latter option was taken here and it is important to observe that the predictive ability of the model is, somewhat, preserved in the present approach. In fact, the *ad hoc* correction was obtained from the static bifurcation analysis and, once defined, it was used here as it stands, with no further corrections.

The parameters of the USP model are those defined in Table 3 of Simos et al (2001), with the friction coefficient C_f being taken equal to the ones measured at IPT wave tank; see Table 2; the Froude correction is applied to the yaw moment coefficient, accordingly to (1), with the factor $k_w(\mathrm{Fr};\psi)$ being defined in Table 3. It is worthwhile to recall that no such Froude correction is necessary in full scale and so, from this point of view, the USP model continues to be entirely predictive for an actual application.

In the ballasted condition the articulation was placed at $a = 0.4$ while the hawser length and towing velocity took again the values $\{(U = 0.4$ m/s; 0.5 m/s; 0.6 m/s); $(L_b/L = 0.1; 0.2; 0.3; \ldots; 1)\}$, totaling, here also, 30 different experiments.

Typical time series for $(\gamma(t); \psi(t); F_H(t))$ are presented in Figs. 12, 13 and 14 for the three velocities and $L_b/L = 0.36$ and 0.70. The agreement between theory and experiment is again fairly good, although for the higher velocity ($U = 0.6$ m/s) the Froude correction seems to give slightly larger values for the amplitude of $\gamma(t)$. It is certainly expected that the simple-minded *ad hoc* correction here proposed should work better when the Froude effect is relatively small, tending to deteriorate if this influence increases.

Results similar to the ones shown in Figs. 12, 13 and 14 can be observed for all cases tested and Fig. 15 displays the overall behavior by showing the amplitudes of $\gamma(t)$ and $\psi(t)$ as functions of L_b/L for the three velocities. The concordance is fair again and particularly for the case $U = 0.5$ m/s one can see the experimental points trying to follow the almost vertical line for the γ-amplitude in the vicinity of the stability border.

5. Conclusion

The hydrodynamic model derived in Simos et al (2001) has been checked in this work against experiments emulating the fishtailing instability that occurs in a single-point moored tanker. In spite of the simplicity of the basic model the concordance is fairly good in general, not only for some overall geometric parameters, such as the amplitudes of the limit-cycles, but also for the finer structures of the related time series. Tests were performed for a

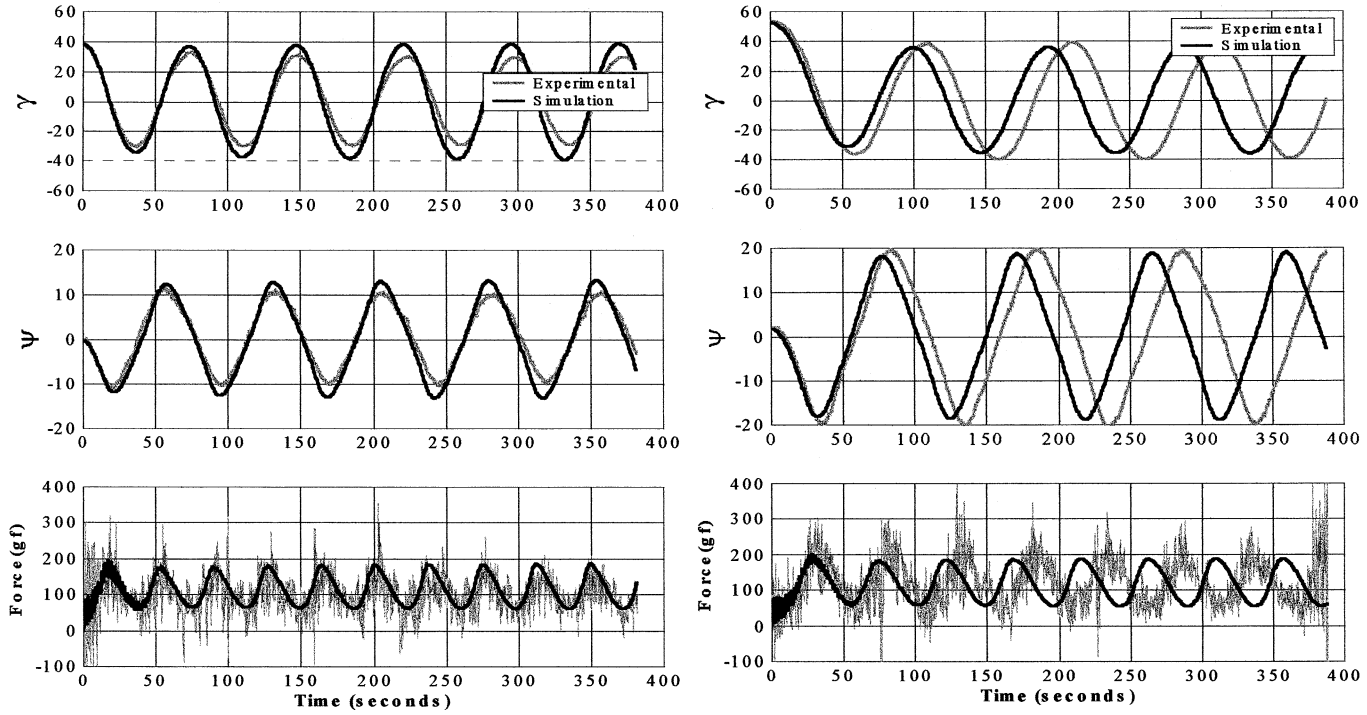

Fig. 12 Fishtailing instability: theory and experiment. VLCC1 ballasted (40%), $U = 0.4$ m/s (USP model corrected by (1) and Table 3)

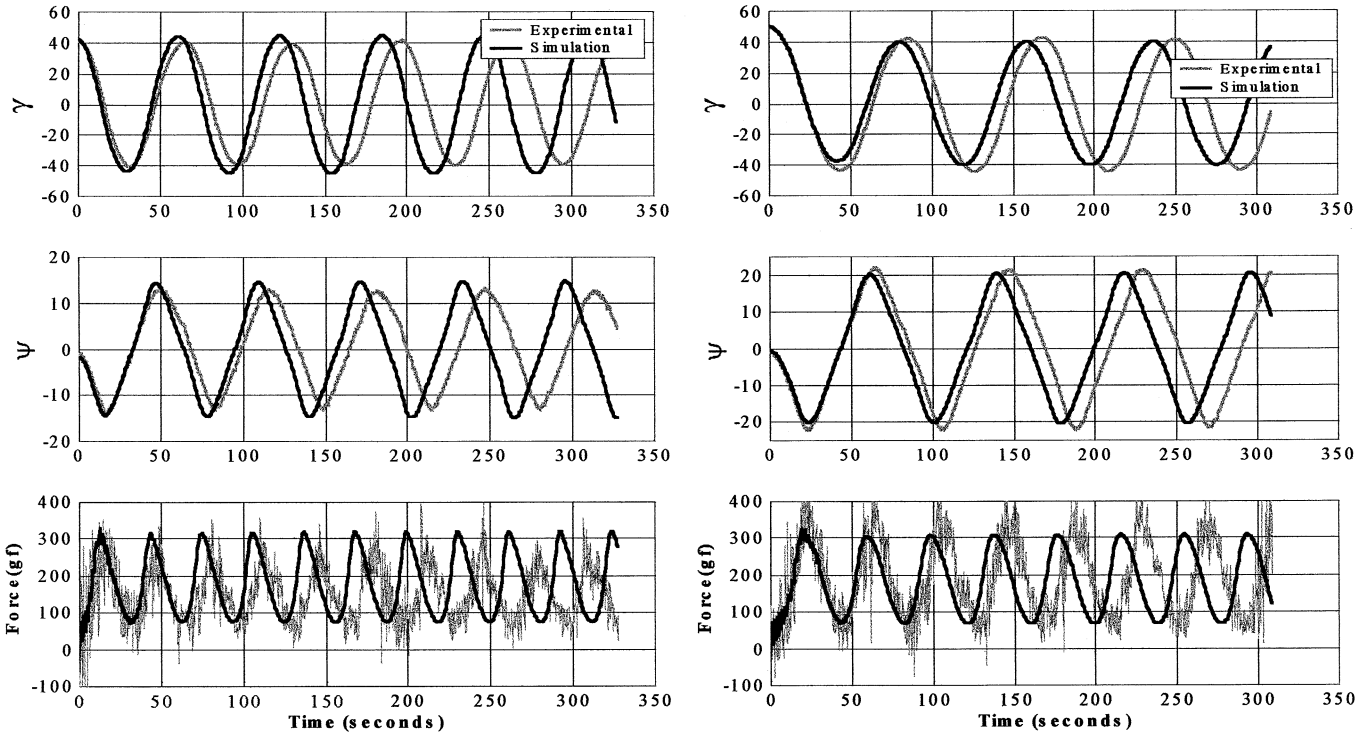

(U = 0.5 m/s; C_f = 0.0335; a = 0.4; L_b/L=0.36; $k_w(Fr;\psi)$ = 0.82)

(U = 0.5m/s; C_f = 0.0335; a = 0.4; L_b/L=0.7 $k_w(Fr;\psi)$ = 0.82)

Fig. 13 Fishtailing instability: theory and experiment. VLCC1 ballasted (40%), $U = 0.5$ m/s (USP model corrected by (1) and Table 3)

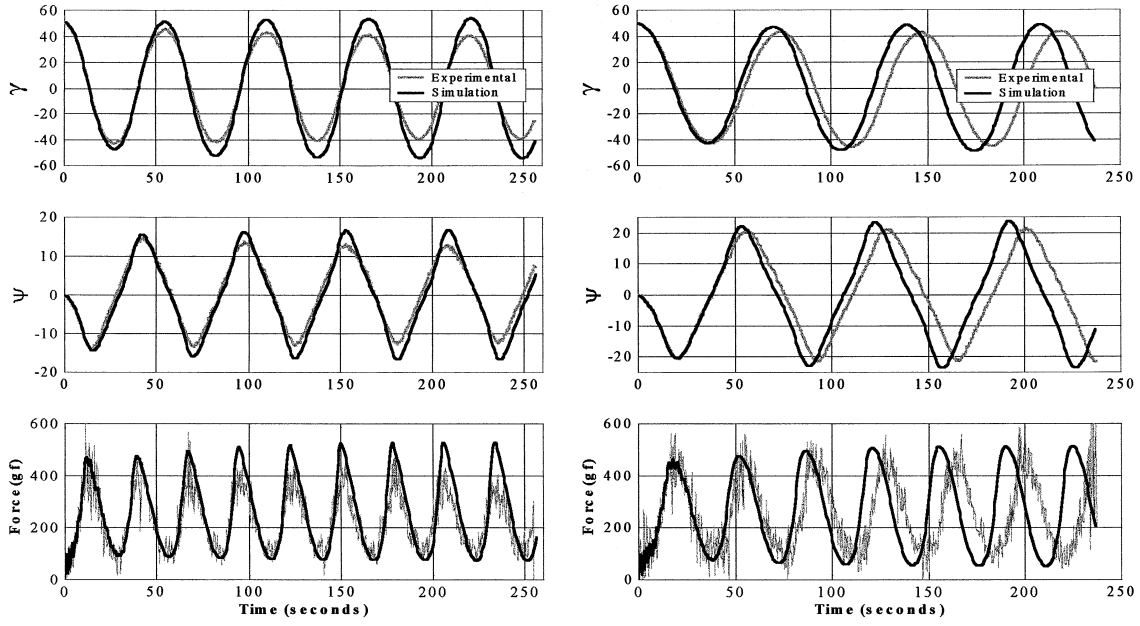

(U = 0.6 m/s; C_f = 0.0320; a = 0.4; L_b/L=0.36; $k_w(Fr;\psi)$ = 1.03)

(U = 0.6 m/s; C_f = 0.0320; a = 0.4; L_b/L=0.7 $k_w(Fr;\psi)$ = 1.03)

Fig. 14 Fishtailing instability: theory and experiment. VLCC1 ballasted (40%), $U = 0.6$ m/s (USP model corrected by (1) and Table 3)

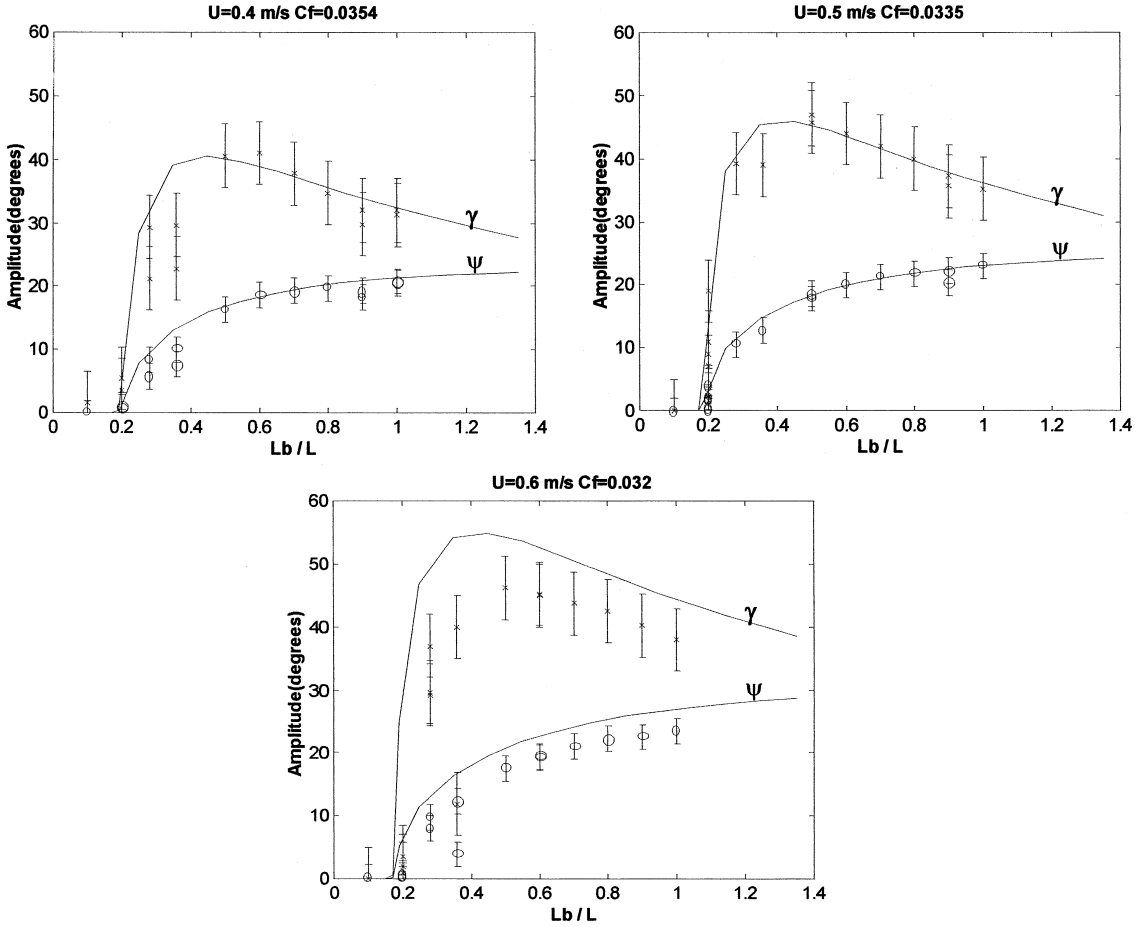

Fig. 15 Amplitude of the limit-cycles as functions of L_b/L—ballasted situation. (+) = $\gamma(t)$—experiment; (o) = $\psi(t)$—experiment; (———)= USP model

very large tanker, both in the loaded and ballasted conditions, but this latter situation deserved a special attention since Froude effect was then relevant. The proposed *ad hoc* correction for this influence seems to be consistent, although a deeper experimental-theoretical analysis would be certainly welcomed in this case. This free-surface influence appears only for relatively high towing velocities, much higher, in general, than the usual ocean current ones; for the typical current velocities the Froude effect is irrelevant and the original model can be directly used in an actual problem.

The comparison with the experimental results was obtained directly with the use of the friction coefficients measured at IPT (see Table 2) and the Froude correction factor inferred from the bifurcation experiments (see Table 3). Some adjustments, within the range of the measured values of the friction coefficient (see Table 2), were sometimes needed in order to obtain a correct fitting for the period. On the other hand, the mathematical model was able to capture even some more subtle behavior of the transient response, as shown in Fig. 8 for $U = 0.6$ m/s, for example.

The derived hydrodynamic model, coined here the USP model, is very simple in conception and, indeed, it has already been proposed, in its essential aspects, by different researches on the field. The emphasis here is not on the model's inherent simplicity, although its *explicit* feature must be stressed, nor on its agreement with the fishtailing experiments, since others models can have this performance too. What is felt to be the important feature of the present model is the coupling between its *simplicity* and its *robustness*, making feasible for one to use the model in order to obtain a reliable response in full scale. The confidence in the mathematical model as an extrapolator is certainly enhanced when it has a simple texture since it must necessarily reflect only the more basic physics of the problem and should hence work as well in full scale. In some aspects, the important point in this paper was to disclose that the apparently intricate fishtailing instability phenomenon depends essentially on some simple physical mechanisms, that can be well described by the ship's main dimensions and a few, and relatively well-known, hydrodynamic coefficients.

This aspect has an even greater importance for a single reason: From the physical understanding of fishtailing phenomenon it was possible to infer, from the outset, the fundamental importance of the *friction coefficient* for the analysis of a single-point moored ship, a conclusion supported by previous works, as the ones presented by Faltinsen (1979) and Jiang & Sharma (1993). It follows, as a consequence, that small-scale experimental results

cannot be used to predict the response of an actual system; only a mathematical model, with a proper correction for the scale effect as the one here derived, would be able to deliver such prediction.

On the other hand, the performance of the ship-hawser system is relatively insensitive to the values of the transverse hydrodynamic coefficients $\{C_Y; lC_Y\}$: One could not detect any sensible difference in the response if these values were taken directly from the measurements or from Hoerner's curve and Table 1 of Simos et al (2001). In this perspective, the USP model in its explicit version seems to be good enough to deal with the fishtailing instability problem.

Finally, the fact that the experiments cannot be extrapolated to full size definitely places an extra responsibility on the mathematical models and a need to give them a more solid empirical background by emulating, in the wave tank, dynamic situations that will be encountered by the actual system in reality. The set of experiments realized in the present work should then be completed by examining different situations such as, for example, the chaotic behavior that may be found when the hawser has a unilateral response and can slacken, or even the dynamic behavior of two ships in a tandem configuration, a situation that can be further complicated by the possible hydrodynamic interaction between them.

Acknowledgments

The authors wish to thank PETROBRAS for supporting the tests conducted at IPT. The first and second authors were supported by FAPESP—The State of São Paulo Research Foundation. The fourth author also acknowledge CNPq Research Fund. Finally, the authors want to thank engineer João V. Sparano for his collaboration.

References

Abkowitz, M. 1964 Lectures on ship hydrodynamics, steering and maneuverability. Hydro-Og Aerodynamisk Laboratorium, Report Hy-5, Lyngby, Denmark, 113.

Clarke, D., Gedling, F., and Hine, G. 1982 The application of maneuvering criteria in hull design using linear theory. *The Royal Institution of Naval Architects*, 45–68.

Faltinsen, O. M., Kjaerland, O., Liapis, N., and Walderhaug, H. 1979 Hydrodynamic analysis of tankers at single-point-mooring systems. *Proceedings*, 2nd International Conference on Behaviour of Off-Shore Structures, BOSS'79, 177–205:

Fucatu, C. and Nishimoto, K. 1998a Desenvolvimento de um simulador dinâmico para análise de navios. Boletim técnico da EPUSP, Dep. de Eng. Naval e Oceânica, BT/PNV/37 (in Portuguese).

Jiang, T. and Sharma, S. D. 1993 Maneuvering simulation of a single-point moored tanker in deep and shallow water. *Proceedings*, International Conference on Marine Simulation and Ship Manoeuvrability, MARSIM'93, 229–241.

Leite, A. J. P., Aranha, J. A. P., Umeda, C., and de Conti, M. B. 1998 Current forces in tankers and bifurcation of equilibrium of turret systems: hydrodynamic model and experiments. *Applied Ocean Research*, **20**, 145–156.

Obokata, J. 1987 On the basic design of single point mooring systems (1st report). *Journal of the Society of Naval Architects of Japan*, **161**, June.

Oltmann, P. and Sharma, S. D. 1984 Simulation of combined engine and rudder maneuvers using an improved model of hull-propeller-rudder interactions. *Proceedings*, 15th Symposium on Naval Hydrodynamics, Hamburg, 83–108.

Simos, A. N., Tannuri, E. A., Pesce, C. P., and Aranha, J. A. P. 2001 A quasi-explicit hydrodynamic model for the dynamic analysis of a moored FPSO under current action. *Journal of Ship Research*, **45**(4), 289–301.

Tabor, M. 1989 *Chaos and Integrability in Nonlinear Dynamics*, John Wiley & Sons, New York.

Takashina, J. 1986 Ship maneuvering motion due to tugs boats and its mathematical model. *Journal of the Society of Naval Architects of Japan*, **160**, Dec.

Wichers, J. E. W. 1987 The prediction of the behavior of single point moored tankers. *Developments in Marine Technology, Floating Structures and Offshore Operations*, **4**, 125–142.